6.5-ns actively Q-switched Nd:YVO_4 laser operating at 1.34 μm

Yongguang Zhao (赵永光)[1], Zhengping Wang (王正平)[1*], Haohai Yu (于浩海)[1], Lei Guo (郭 磊)[1], Lijuan Chen (陈丽娟)[1], Shidong Zhuang (庄世栋)[1,3], Xun Sun (孙 洵)[1], Dawei Hu (胡大伟)[2], and Xinguang Xu (许心光)[1]

[1]*State Key Laboratory of Crystal Materials and Institute of Crystal Materials, Shandong University, Ji'nan 250100, China*

[2]*Institute of Science Technology for National Defence, Shandong University, Ji'nan 250100, China*

[3]*School of Science, Shandong Jianzhu University, Ji'nan 250101, China*

[*]*Corresponding author: zpwang@sdu.edu.cn*

Received February 17, 2011; accepted March 15, 2011; posted online May 31, 2011

With a plano-concave cavity, diode-pumped continuous-wave (CW) and actively Q-switched Nd:YVO_4 laser operating at 1.34 μm is demonstrated. Maximum CW output power of 4.76 W and Q-switched average output power of 2.64 W are obtained with output coupler (transmission $T = 3.9\%$). For the Q-switching operation, the theoretically calculated pulse energy and pulse width, with a pulse repetition frequency (PRF) range of 5–40 kHz, coincide with the experimental results. With a $T = 11.9\%$ output coupler, the maximum peak power of 24.3 kW and minimum pulse width of 6.5 ns are obtained when the PRF is 10 kHz. To the best of our knowledge, this is the shortest actively Q-switched pulse duration ever obtained in a 1.3-μm Nd-doped vanadate laser.

OCIS codes: 140.3480, 140.3530, 140.3540, 140.3580.

doi: 10.3788/COL201109.081401.

Diode pumped solid-state lasers (DPSSLs) approximately 1.3 μm have attracted much attention in recent years because of their potential applications in medicine, fiber optics, spectroscopy, etc. Among well-developed Nd-doped vanadate crystals such as Nd:YVO_4[1−4], Nd:$LuVO_4$[5,6], and Nd:$GdVO_4$[7−9], Nd:YVO_4 has been recognized as the optimum material to produce 1.3-μm laser output because its stimulated emission cross-section for the $^4F_{3/2} \rightarrow {}^4F_{13/2}$(1.34 μm) transition is the largest. Moreover, the ratio of fluorescence radiation intensity of Nd:YVO_4 at 1.34–1.06 μm is approximately 0.24, which is much greater than the other two Nd-doped vanadates. These characteristics mean that compared with Nd:$LuVO_4$ or Nd:$GdVO_4$, continuous-wave (CW) or Q-switched 1.34-μm laser can be more conveniently constructed with a Nd:YVO_4 crystal. With a V^{3+}:YAG as the saturable absorber, Agnesi *et al.* obtained a 0.7-μJ pulse energy of passively Q-switched mode-locking at the repetition rates of 10–50 kHz by a diode-pumped Nd:YVO_4 laser[10]. An acousto-optical (A-O) Q-switched 1.34-μm laser with double Nd:YVO_4 crystals pumped by fiber-coupled laser diodes (LDs) was presented by Lu *et al.*, in which at 10-kHz repetition rate, the shortest pulse width was 19 ns and the peak power was higher than 30 kW[11]. In this letter, we demonstrate efficient single-end diode-pumping CW and A-O Q-switched Nd:YVO_4 lasers operating at 1.34 μm. For Q-switched operation, the theoretical calculated results coincided with the experimental data. When the output coupler transmission was 11.9%, the pulse width and the peak power were 6.5 ns, 24.3 kW at a pulse repetition frequency (PRF) of 10 kHz, and 14.8 ns, 3.9 kW at a PRF of 40 kHz, respectively.

The experimental setup is shown in Fig. 1. Previous researches have shown that, for 1.34-μm operation, low Nd^{3+} doping concentration of Nd:YVO_4 crystal presents higher slop efficiency because of the small Auger up conversion process. The reduced absorption coefficient at the incident pump power for low doping could decrease thermal loading in the laser crystal and increase achievable output power; the optimum value for the Nd^{3+} doping concentration was determined to be in the 0.25–0.5 at.-% range[12−14]. Thus, in the current experiment, we chose an a-cut Nd:YVO_4 crystal with 0.3 at.-% Nd^{3+} concentration and 3 × 3 × 10 (mm) dimension. Both end surfaces of the laser crystal were anti-reflection (AR) coated at 808, 1064, and 1342 nm, and the reflectivity of 1064 nm was limited to < 0.3% to ensure that radiation would not oscillate. The pump source was a fiber-coupled LD with a central wavelength of approximately 808 nm. The core diameter and the numerical aperture (NA) of the fiber bundle were 1.55 and 0.22 mm, respectively. Using a 3:1 focusing system, the pump source output was focused into the laser crystal with a spot radius of 0.258 mm. The absorption efficiency of Nd:YVO_4 crystal to the pump light was

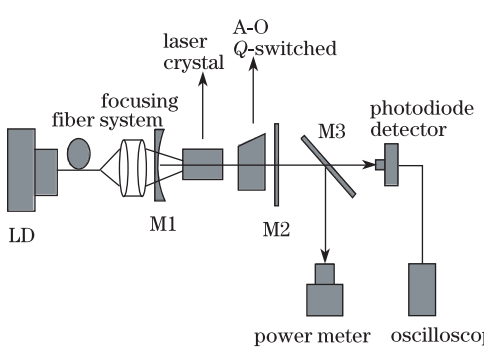

Fig. 1. Schematic diagram of the experimental laser setup.

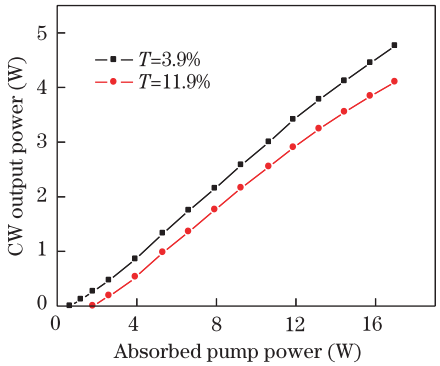

Fig. 2. CW output power at 1.34 μm as a function of the absorbed pump power.

~92%. M1 was the input mirror with a curvature radius of 200 mm, which was high-transmission (HT) coated at 808 nm, 1.06 μm on the flat face, and HT coated at 808 nm, 1.06 μm and high-reflection (HR) coated at 1.34 μm on the concave face. The output couplers, M2, were flat mirrors with different transmissions (T = 3.9% and 11.9%) at 1.34 μm. A 1.34 μm, A-O Q-switch was inserted between the laser crystal and the output coupler. The physical length of the concave-flat cavity was 1.3 cm for the CW laser experiments, and the cavity length was lengthened to 7.4 cm for Q-switched operation. The generated CW and average output power was measured by an energy/power meter (EPM 2000, Molectron Inc.). The temporal behaviors of the Q-switched laser were recorded by a DPO7104 digital oscilloscope (1-GHz bandwidth and 10-Gs/s sampling rate, Tektronix Inc.). To remove the generated heat under high pump power levels, the laser crystal was wrapped with indium foil and mounted in a water-cooled copper block, and the A-O Q-switch was mounted on another water-cooled copper block. The temperature of cooling water was controlled at 15 °C.

The 1.34-μm CW laser experiment with a cavity length of 1.3 cm was carried out. The CW output power, as a function of the absorbed pump power, is shown in Fig. 2. With T = 3.9% output coupler, the maximum output power was 4.76 W under an absorbed pump power of 17 W, resulting in an optical conversion efficiency of 28% and a slop efficiency of 29.1%. The physical length of the laser resonator was adjusted to 7.4 cm and the A-O Q-switch was inserted to carry out the 1.34-μm pulse laser experiment. For T = 3.9% output coupler, Fig. 3

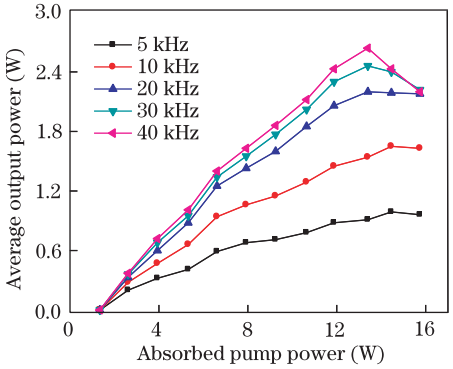

Fig. 3. Dependence of the average output power on the absorbed pump power at different PRFs (T = 3.9%).

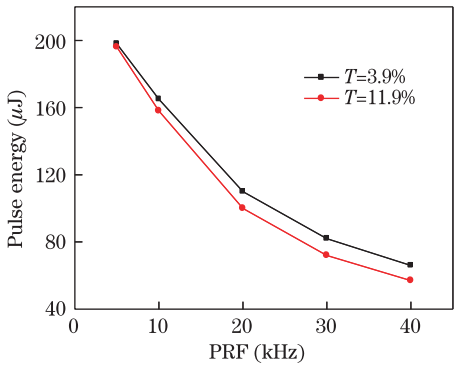

Fig. 4. Variation of pulse energy with PRF.

shows the dependence of the average output power on the absorbed pump power at different PRFs. During high PRFs of 30 and 40 kHz, the output power dropped off rapidly after it reached the maximum value at a high pump power of 13.4 W. During low PRFs of 5–20 kHz, the maximum value of output power could be maintained in the pump range of 13.4–15.6 W. We supposed that this phenomenon was caused by the thermal effect discrepancy of the A-O Q-switch. Figure 3 shows that, at high pump level, the output power of high PRF is much

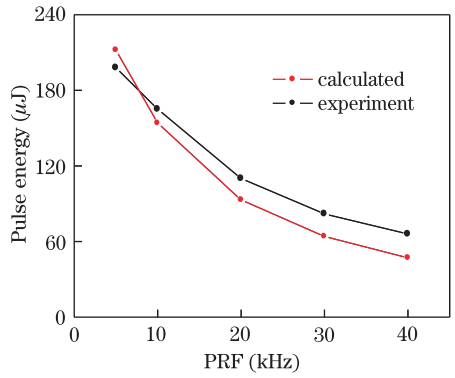

Fig. 5. Experimental data and calculated results of pulse energy.

Table 1. Parameters Used in Theoretical Calculations of Pulsd Energy and Pulse Width

τ	110 μs
η	0.92
$P_{\rm th}$	1.3 W
σ	1.59×10^{-19} cm^2
l	1 cm
ξ	0.98
r_1	0.96
r_2	1
β	0.02 cm^{-1}
w	0.022 cm
L	7.4 cm
$h\nu$	1.48×10^{-19} J
δ	0.86
$n_{\rm th}$	3.8×10^{17} cm^{-3}
$P_{\rm in}$	15 W

Table 2. Calculated Results of n_0, n_f, and Pulse Width

PRF	5 kHz	10 kHz	20 kHz	30 kHz	40 K
n_0 (cm^{-3})	3.4×10^{18}	2.4×10^{18}	1.5×10^{18}	1.1×10^{18}	0.82×10^{18}
n_f (cm^{-3})	0.03×10^{16}	0.3×10^{16}	2.7×10^{16}	6×10^{16}	8.8×10^{16}
t_{cal} (ns)	13	15	20	28	40
t_{exp} (ns)	15	12	17	19	21

larger than that of low PRF; thus, the intra-cavity circulation laser power will be very large for high PRF, especially when a small transmission mirror is used as the output coupler. As a result, high PRF operation had severe thermal effects on Q-switch, making the cavity unstable and the output power drop off easily. Figure 4 shows the variation of pulse energy with the PRF, where the pulse energy decreased rapidly as the PRF changed from 5 to 40 kHz. The maximum pulse energy was 198 μJ, obtained at 5 kHz with $T = 3.9\%$ output coupler.

According to the theory of LD end-pumped actively Q-switched solid-state lasers[15], the single pulse energy can be expressed as

$$E = (n_0 - n_f)h\nu V\sigma_0, \tag{1}$$

where $n_0 = K\tau P_{in}(1 - e^{-1/f\tau})$, τ is the fluorescent lifetime, P_{in} is the incident pump power, and f is the PRF. K is a pumping constant and can be determined through the relation $K = \eta n_{th}/\tau P_{th}$, where η is the absorption efficiency, P_{th} is the threshold pump power, and n_{th} is the threshold inversion density, which can be calculated from the equation[16]: $n_{th} = \frac{1}{\sigma}[\frac{1}{l}\ln(\xi\sqrt{r_1 r_2})^{-1} + \beta]$. In this relation, σ is the stimulated emission cross-section and can be calculated according to Ref. [17], l is the length of the laser crystal, ξ is the single pass transmission, r_1 and r_2 are the reflectances of the output couple and the rear mirror, respectively, and β is the loss coefficient of the laser crystal. n_f can be obtained by the relation: $n_f = n_0 e^{-n_0 l\sigma/\gamma}$, of which $\gamma = 1 - \xi\sqrt{r_1 r_2}e^{-\beta l}$ is a cavity loss factor.

V is the effective lasing volume and can be given by $V = \pi w^2 l\delta$, where w is the fundamental mode radius, and δ is introduced to account for the reduction in the lasing volume resulting from the end-pumping geometry.

σ_0 is the fraction of circulating laser radiation within the resonant cavity that emerges as useful output. The value of the coupling factor σ_0 is given by

$$\sigma_0 = \frac{\ln(r_1)}{\ln(\xi^2) + \ln(r_1) + \ln(r_2) - 2\beta l}. \tag{2}$$

The pulse width can be estimated approximately by

$$t_{cal} = \frac{2L/c}{1 - \ln(r_1) - \xi}\frac{n_0 - n_f}{n_0 - n_{th}[1 + \ln(n_0/n_f)]}. \tag{3}$$

All the parameters used to calculate the pulse energy and the pulse width are listed in Table 1. Figure 5 shows the comparison of the experimental data with the calculated results on pulse energy for the $T = 3.9\%$ output coupler. The two curves exhibited a rough agreement, in which both demonstrated that high pulse energy could be obtained at low PRF. The calculated and measured pulse widths are shown in Table 2. At low PRF, the theoretical value coincided well with the corresponding experimental value, whereas there was evident discrepancy when PRF was greater than 30 kHz. This occurrence could be attributed to the calculating assumption that both inversion and photon density remain uniform across the transverse section of the laser crystal. Although this assumption does not lead to serious error in the calculation of pulse energy, it limits the calculating accuracy of pulse formative time and pulse width[15,16].

With the relation of $P_{peak} = E/t$, we can obtain the peak power of Q-switched pulse, where E is the pulse energy and t is the pulse width. Figures 6 and 7 show the dependence of pulse width and peak power on PRF, respectively. With a $T = 11.9\%$ output coupler, the maximum peak power of 24.3 kW and the minimum pulse width of 6.5 ns were obtained at a PRF of 10 kHz. The corresponding pulse waveform and pulse train are shown in Fig. 8. Figures 4, 6, and 7 show that, for A-Q, actively Q-switching low PRF (< 10 kHz) is favorable for obtaining high peak power because of the large pulse energy and the narrow pulse width.

For comparison, we examined the 1.34-μm A-O Q-switched performance of an a-cut 0.5 at.-% Nd:YVO_4 crystal with the same experimental setup. The results were much inferior to that of 0.3 at.-% Nd:YVO_4 crystal reported above. The maximum single pulse energy,

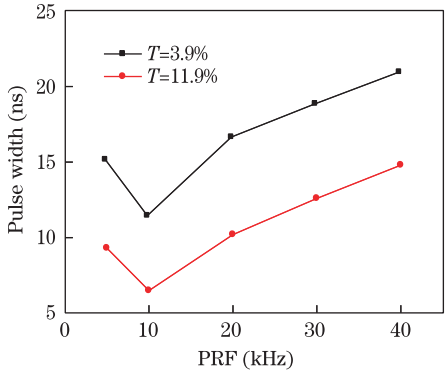

Fig. 6. Dependence of pulse width on PRF.

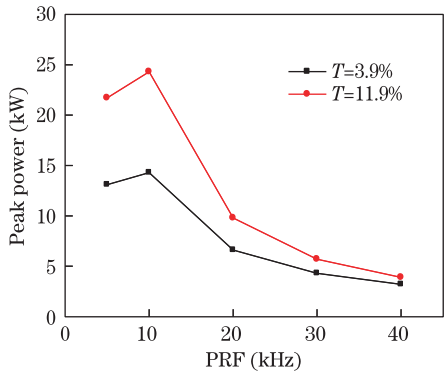

Fig. 7. Dependence of peak power on PRF.

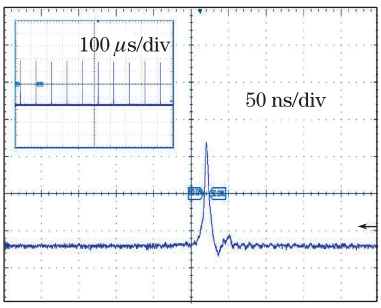

Fig. 8. Pulse waveform of 6.5 ns (inser: corresponding pulse train of 10 kHz)

shortest pulse width, and highest peak power, which were 78 μJ, 12.9 ns, 6.1 kW for the $T = 3.9\%$ output coupler and 112 μJ, 23.8 ns, 4.7 kW for the $T = 11.9\%$ output coupler, were achieved at a PRF of 5 kHz.

In conclusion, short pulse width is significant to diode-pumped actively Q-switched lasers. Previous research have shown that, at high PRF, the average output power of actively Q-switched lasers will approach CW output power with the same cavity structure[18,19], which is determined mainly by the inherent characteristic of the laser material. Hence, in high PRF operations of such lasers, the single pulse energy is limited. Thus, in this situation, decreasing the pulse width is the key method for enhancing the peak power. In this letter, actively Q-switched Nd:YVO_4 laser at 1.34 μm obtains short pulse width and high peak power by shortening the laser cavity and choosing the laser material properly. When the transmission of output coupler is 11.9%, the pulse width and the peak power are 6.5 ns, 24.3 kW at a PRF of 10 kHz, and 14.8 ns, 3.9 kW at a PRF of 40 kHz, respectively. To the best of our knowledge, this is the shortest actively Q-switched pulse duration ever obtained in a 1.3-μm Nd-doped vanadate laser. The compact structure, efficient output, and excellent pulse performance are favorable for future applications in relevant fields.

This work was supported by the National Natural Science Foundation of China (No. 60978027), the Natural Science Foundation of Shandong Province (Nos. 2009ZRB01907 and ZR2010EM001), the Program for New Century Excellent Talents in University (No. NCET-10-0526), and the Independent Innovation Foundation of Shandong University (Nos. 2009TS129, 2010JC015, and 2010TS090).

References

1. H. Ogilvy, M. J. Withford, P. Dekker, and J. A. Piper, Opt. Express **11,** 2411 (2003).
2. X. Ding, H. Zhang, R. Wang, W. Q. Wen, P. Wang, J. Q. Yao, and X. Y. Yu, Opt. Express **16,** 11247 (2008).
3. X. Yu, F. Chen, R. Yan, X. Li, J. Yu, and Z. Zhang, Chin. Opt. Lett. **8,** 499 (2010).
4. W. Wang, J. Liu, F. Chen, L. Li, and Y. Wang, Chin. Opt. Lett. **7,** 706 (2009).
5. F. Liu, J. He, B. Zhang, J. Xu, X. Dong, K. Yang, H. Xia, and H. Zhang, Opt. Express **16,** 11759 (2008).
6. Y. F. Lv, X. H. Zhang, J. F. Chen, G. C. Sun, and Z. M. Zhao, Laser Phys. Lett. **7,** 699 (2010).
7. W. Ge, H. Zhang, J. Wang, X. Cheng, and M. Jiang, Opt. Express **13,** 3883 (2005).
8. J. Liu, B. Ozygus, S. Yang, J. Erhard, U. Seelig, A. Ding, and H. Weber, J. Opt. Soc. Am. B **20,** 652 (2003).
9. K. Yang, S. Zhao, J. He, B. Zhang, C. Zuo, G. Li, D. Li, and M. Li, Opt. Express **16,** 20176 (2008).
10. A. Agnesi, A. Guandalini, G. Reali, J. Jabczynski, K. Kopczynski, and Z. Mierczyk, Opt. Commun. **194,** 429 (2001).
11. C. Lu, M. Gong, L. Huang, and F. He, Appl. Phys. B **89,** 285 (2007).
12. H. Zhang, J. Liu, J. Wang, C. Wang, L. Zhu, Z. Shao, X. Meng, X. Hu, Y. Chow, and M. Jiang, Opt. Lasers Eng. **38,** 527 (2002).
13. Y. F. Chen, L. J. Lee, T. M. Huang, and C. L. Wang, Opt. Commun. **163,** 198 (1999).
14. Y.-F. Chen, IEEE J. Quantum Electron. **35,** 234 (1999).
15. J. Liu, C. Wang, C. Du, L. Zhu, H. Zhang, X. Meng, J. Wang, Z. Shao, and M. Jiang, Opt. Commun. **188,** 155 (2001).
16. G. D. Baldwin, IEEE J. Quantum Electron. **QE-7,** 220 (1971).
17. N. Mermilliod, R. Romero, I. Chartier, C. Garapon, and R. Moncorge, IEEE J. Quantum Electron. **28,** 1179 (1992).
18. J. Liu, B. Ozygus, J. Erhard, A. Ding, H. Weber, and X. Meng, Opt. Quant. Electron. **35,** 811 (2003).
19. J. Liu, H. Zhang, Z. Wang, J. Wang, Z. Shao, M. Jiang, and H. Weber, Opt. Lett. **29,** 168 (2004).